

Experimental Treatment of SIV-Infected Macaques via Autograft of CCR5-Disrupted Hematopoietic Stem and Progenitor Cells

Songlin Yu,^{1,2,3,4} Yang Ou,³ Hongkui Xiao,⁴ Jiaojiao Li,⁴ Dickson Adah,⁴ Shiquan Liu,³ Siting Zhao,⁴ Li Qin,⁴ Yongchao Yao,⁴ and Xiaoping Chen⁴

¹Department of Hematology and Key Laboratory of Non-resolving Inflammation and Tumor, The Third Xiangya Hospital, Central South University, Changsha, Hunan Province 410000, P. R. China; ²Postdoctoral Research Station of Clinical Medicine, the Third Xiangya Hospital, Central South University, Changsha, Hunan Province, 410000 P. R. China; ³Hunan Provincial Key Laboratory of Dark Tea and Jin-hua, School of Materials and Chemical Engineering, Hunan City University, Yiyang, Hunan Province 413099, P. R. China; ⁴State Key Laboratory of Respiratory Disease, Center of Infection and Immunity, Guangzhou Institutes of Biomedicine and Health (GIBH), Chinese Academy of Sciences, Guangzhou, Guangdong Province 510530, P. R. China

Hematopoietic stem cell (HSC)-based gene therapy targeting CCR5 represents a promising way to cure human immunodeficiency virus type 1 (HIV-1) infection. Yet the preclinical animal model with transplantation of autologous CCR5-ablated HSCs remains to be optimized. In this study, four Chinese rhesus macaques of simian immunodeficiency virus (SIV) chronic infection were given long-term antiretroviral therapy (ART), during which peripheral CD34⁺ hematopoietic stem and progenitor cells (HSPCs) were purified and infected with CCR5-specific CRISPR/Cas9 lentivirus (three monkeys) or GFP lentivirus (one monkey). After non-myeloablative conditioning, the CCR5-modified or GFP-labeled HSPCs were autotransplanted to four recipients, and ART was withdrawn following engraftment. All of the recipients survived the process of transplantation. The purified CD34⁺ HSPCs harbored an undetectable level of integrated SIV DNA. The efficiency of CCR5 disruption in HSPCs ranges from 6.5% to 15.6%. Animals experienced a comparable level of hematopoietic reconstruction and displayed a similar physiological homeostasis. Despite the low-level editing of CCR5 *in vivo* (0.3%–1%), the CCR5-disrupted cells in peripheral CD4⁺ Effector Memory T cell (TEM) subsets were enriched 2- to 3-fold after cessation of ART. Moreover, two of the three treated monkeys displayed a delayed viral rebound and a moderately recovered immune function 6 months after ART withdrawal. This study highlights the importance of improving the CCR5-editing efficacy and augmenting the virus-specific immunity for effective treatment of HIV-1 infection.

INTRODUCTION

Acquired immune deficiency syndrome (AIDS) caused by human immunodeficiency virus type 1 (HIV-1) is a hard-to-cure chronic infectious disease. In 2007, a HIV-1-infected man who suffered from acute myeloid leukemia received transplantation of bone marrow from a donor who was homologous for a natural deletion of 32 bp within CCR5 gene (CCR5 Δ 32/ Δ 32).^{1,2} More recently, another HIV-1-in-

fecting individual underwent transplantation of CCR5 Δ 32/ Δ 32 hematopoietic stem cells (HSCs) to treat Hodgkin's lymphoma.³ These patients are both identified free of any detectable HIV-1 and remain healthy until now. It was demonstrated that the CCR5 Δ 32/ Δ 32 genotype played a key role in both cases.^{4–6} However, wide application of this success is limited by the rare population of people with natural CCR5 Δ 32/ Δ 32 genotype, as well as the restriction of histocompatibility leukocyte antigen (HLA) match.⁷ Accordingly, autograft of engineered CCR5-ablated HSCs from infected patients would provide an alternative treatment that may lead to the functional cure of AIDS.⁸

Advances in genome editing have brought significant progress in disease curing. CRISPR/Cas9, as a simple and efficient gene-editing tool, has been extensively applied to construct gene knockout animals, treat the genetic disorders, as well as develop new strategies for HIV-1 gene therapy.^{9–11} Mandal et al.¹² co-transfected Cas9 expression vector and CCR5-sgRNA (single guide RNA) into human CD34⁺ hematopoietic stem and progenitor cells (HSPCs) by nuclear transfection and obtained a 42% knockout efficiency. Recently, Xu et al.¹³ transplanted the CRISPR-mediated CCR5-

Received 28 February 2020; accepted 10 March 2020;
<https://doi.org/10.1016/j.omtm.2020.03.004>.

Correspondence: Songlin Yu, State Key Laboratory of Respiratory Disease, Center of Infection and Immunity, Guangzhou Institutes of Biomedicine and Health (GIBH), Chinese Academy of Sciences, 190 Kaiyuan Avenue, Guangzhou Science Park, Guangzhou, Guangdong Province 510530, P. R. China.

E-mail: yu_songlin@gibh.ac.cn; yxl_xy3@163.com

Correspondence: Yongchao Yao, State Key Laboratory of Respiratory Disease, Center of Infection and Immunity, Guangzhou Institutes of Biomedicine and Health (GIBH), Chinese Academy of Sciences, 190 Kaiyuan Avenue, Guangzhou Science Park, Guangzhou, Guangdong Province 510530, P. R. China.

E-mail: yaoyongchao@szu.edu.cn

Correspondence: Xiaoping Chen, State Key Laboratory of Respiratory Disease, Center of Infection and Immunity, Guangzhou Institutes of Biomedicine and Health (GIBH), Chinese Academy of Sciences, 190 Kaiyuan Avenue, Guangzhou Science Park, Guangzhou, Guangdong Province 510530, P. R. China.

E-mail: chen_xiaoping@gibh.ac.cn



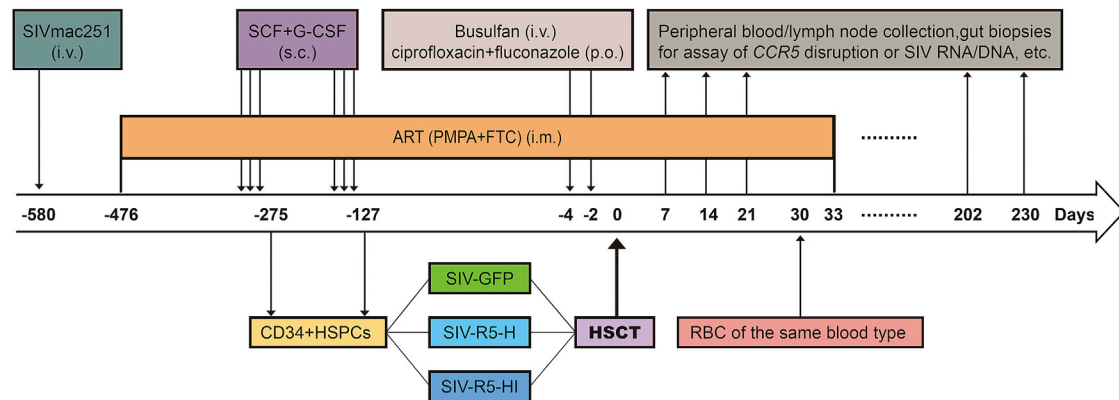


Figure 1. Animals and the Experimental Design

A schematic diagram of the animal experiment. Chinese rhesus macaques were inoculated with SIVmac251 and treated with ART for over 1 year. The ART regimen (PMPA and FTC) was administered i.m. once daily. During the ART treatment, SCF and G-CSF were subcutaneously (s.c.) injected to mobilize HSPCs to peripheral blood before apheresis. Two collections of CD34⁺ HSPCs were pooled together and infected with SIV-GFP, SIV-R5-H, or SIV-R5-HI. After conditioning with busulfan, the CCR5-modified HSPCs were autotransplanted to SIV-infected monkeys. ART was terminated when the engraftment was successful. The virological and immunological indicators, as well as the physiological status of monkeys, were monitored at multiple time points before and after transplantation.

disrupted HSCs into a HIV-1-infected man with acute lymphocytic leukemia. Despite the long-term engraftment of CCR5-ablated HSPCs, the viral rebound was observed upon interruption of antiretroviral therapy (ART).¹³ Considering the relatively low efficiency of gene modification *in vivo*, it remains challenging for application of CRISPR in HIV-1 treatment.¹⁴ As an alternative method to deliver therapeutic genes, lentiviruses have been widely used for treating the genetic disorders, as well as HIV-1 infection.^{15–17} We and others have successfully deleted the CCR5 gene in CD4⁺ T cells via the lentivirus-vectored CRISPR/Cas9 and supplied protection to the modified CD4⁺ T cells.^{18–20} However, this strategy still needs *in vivo* validation in patients who have been infected with HIV-1.

Rhesus macaque is an ideal model for AIDS research owing to its similar genetic background, disease course, and pathological features to humankind.²¹ We and others have established the chronic simian immunodeficiency virus (SIV) infection model in rhesus monkeys.^{22–24} Recently, Peterson et al.^{25,26} conducted high-level CCR5 editing in monkey CD34⁺ HSPCs utilizing zinc finger nucleases (ZFNs) and engrafted the modified autologous HSPCs to SIV-infected recipients. Although yielding a CCR5 disruption frequency of ~4% in peripheral blood, this treatment could not repress the viral rebound after withdrawal of ART.²⁶ In this study, we constructed a SIV-based CRISPR-CCR5/Cas9 lentivirus to disrupt the CCR5 gene in HSPCs collected from SIV-infected macaques. The modified autologous HSPCs were engrafted back to the infected monkeys under the non-myeloablative conditioning. The virological and immunological indicators, as well as gene modification efficiencies, were monitored at multiple time points before and after transplantation. This study might help to further verify the concept of utilizing autologous HSCs with customized CCR5 deficiency to cure HIV-1 infection.

RESULTS

The CCR5 Gene in Monkey HSPCs Was Disrupted by Lentivirus-Delivered CRISPR/Cas9

To determine the optimal time for mobilization, two normal rhesus monkeys (RM G06066 and RM S02169) were given stem cell factor (SCF) and granulocyte-colony stimulating factor (G-CSF) for 5 consecutive days according to previous research;²⁴ the proportion of CD34⁺ HSPCs in peripheral blood increased on the first day and came to the highest percentage on the third day of mobilization (from 14% to 25% for RM G06066 and from 15% to 22% for RM S02169). Hence four SIV-infected rhesus monkeys (RM 31, RM 27, RM C3, and RM 34) were subjected to apheresis on the third day of mobilization (Figure 2A). The ratio of enriched CD34⁺CD38[−] HSPCs, which are defined as the key feature of true HSCs,²⁷ was measured before and after sorting (~10% versus ~73%) (Figure 2B). Statistically, the purity of CD34⁺ HSPCs after sorting was about 70% (69.74% ± 12.83%), whereas that of CD34⁺CD38[−] HSPCs was ~51% (51.60% ± 12.56%) (Figure 2C).

In a previous study, we screened two optimal guide RNAs (sgR5-H and sgR5-I) targeting the CCR5 conserved sequence among human and rhesus; the off-target events were not detectable in both the monkey Vero cell line and HSPCs after transfection of sgR5-H and/or sgR5-I according to non-homologous end joining (NHEJ) assay and Sanger sequencing.^{9,19} Accordingly, we constructed two SIV-based lentiviruses: SIV-R5-H, which harbors sgRNA, and SIV-R5-HI, which holds dual guide RNAs targeting diverse locus for predictable deletion of CCR5.¹² SIV-R5-H or SIV-R5-HI was used to infect the purified CD34⁺ HSPCs from SIVmac251-infected monkeys in the treated group, and the control vector SIV GFP was used to infect the purified CD34⁺ HSPCs from an SIVmac251-infected monkey in the control group as shown in Figure 1. The transfection efficiency was qualitatively assessed by GFP-based

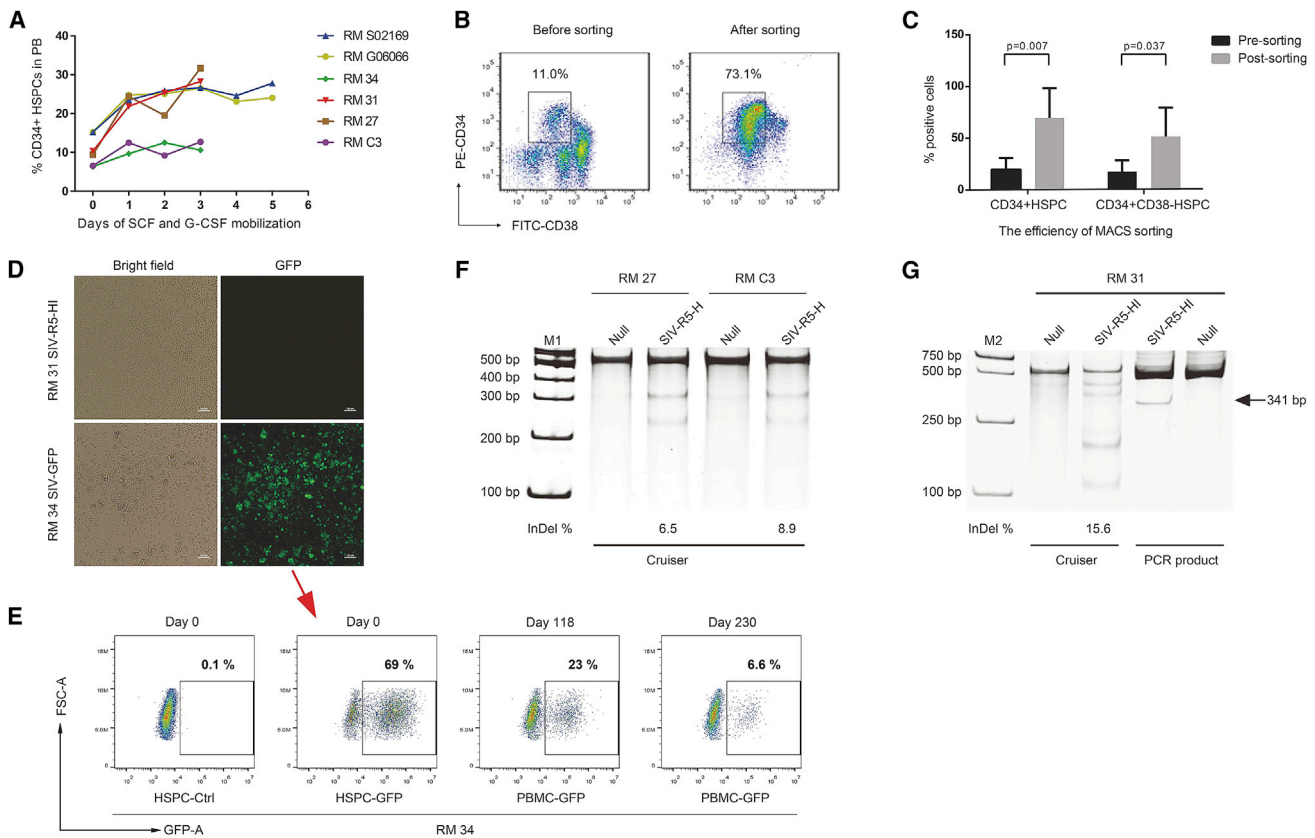


Figure 2. The *CCR5* Gene in $CD34^+$ HSPCs Was Efficiently Disrupted by Lentivirus-Vectored CRISPR/Cas9

(A) The percentage of $CD34^+$ HSPCs in peripheral blood (PB) after mobilization. Four SIV-infected and two normal rhesus monkeys were given SCF and G-CSF for 3 and 5 days, respectively. (B) Representative FACS dot diagram of the proportion of $CD34^+CD38^-$ HSPCs before and after magnetic activated cell sorting (MACS) sorting. (C) The statistical analysis of the $CD34^+$ HSPCs and $CD34^+CD38^-$ HSPCs in four SIV-infected animals before and after sorting. Data are expressed as mean \pm SD with p values indicated in the histogram. (D) Representative fluorescence image of SIV-GFP- and SIV-R5-HI-infected $CD34^+$ HSPCs. Scale bars, 100 μ m. (E) The proportion of GFP⁺ cells in infusion HSPCs or in peripheral blood was quantitatively determined by FACS at indicated time points before and after transplant. The red arrow indicates the correspondence of fluorescence image to the quantitative data obtained by FACS at the day of transplantation (day 0). (F and G) NHEJ assay for *CCR5* gene modification in $CD34^+$ HSPCs after transduction with SIV-R5-H for RM 27 and RM C3 (F) and SIV-R5-HI for RM 31 (G) at an MOI of 100. The 341-bp band (marked by a black arrow) indicates the intended deletion of 252 bp between Cas9 sites for the sgR5-H and sgR5-I (F). Cruiser indicates the PCR products that underwent Cruiser digestion. PCR product indicates the PCR products without treatment of Cruiser. Marker M1, 100-bp DNA ladder; M2, DL2000 DNA marker.

fluorescence microscopy (Figure 2D) and quantitatively determined by fluorescence-activated cell sorting (FACS) gating of GFP⁺ cells at indicated time points before and after transplant (Figure 2E). The percentage of GFP⁺ cells in HSPC infusion products was nearly 70%. Following transplant, the ratio of GFP⁺ cells in peripheral blood decreased over time and dropped to 6.6% 8 months later (Figure 2E), which was similar to previous research.²⁸ The efficiency of *CCR5* modification in HSPCs challenged with SIV-R5-H was 6.5% for RM 27 and 8.9% for RM C3, respectively (Figure 2F). Specifically, the efficiency of *CCR5* disruption in HSPCs treated with SIV-R5-HI was up to 15.6% (RM 31) (Figure 2G). More importantly, there was about 5% of HSPCs infected with SIV-R5-HI showing a targeted ablation of a specific 252-bp sequence in *CCR5* locus (Figure 2G). Collectively, these data demonstrated that both sgRNA- and dual guide RNA-directed Cas9 could result in the disruption of *CCR5* in monkey $CD34^+$ HSPCs.

The Multilineage Potential of *CCR5*-Modified Monkey HSPCs and the *In Vivo* Dynamics of Different Hematopoietic Cell Subsets

To determine whether the treatment of CRISPR/Cas9 lentiviruses affected the multilineage potential of monkey HSPCs, we performed an *in vitro* colony formation assay. The *CCR5*-modified HSPCs could differentiate into macrophages, granulocytes, erythrocytes, and megakaryocyte lineages regardless of whether sgRNAs, dual guide RNAs, or no guide RNAs were applied (Figure 3A). The proportion of CFU-granulocyte/macrophage (CFU-GM) was the largest among all the colony-forming units (CFUs) (Figure 3B). Next, we assessed the dynamics of different hematopoietic cell subsets before and after transplantation. The number of total white blood cells (WBCs) declined drastically after injection of busulfan and began to recover slowly 11–23 days postengraftment (Figure 3C). For neutrophil (NEU), the absolute count decreased markedly after injection of busulfan and began to

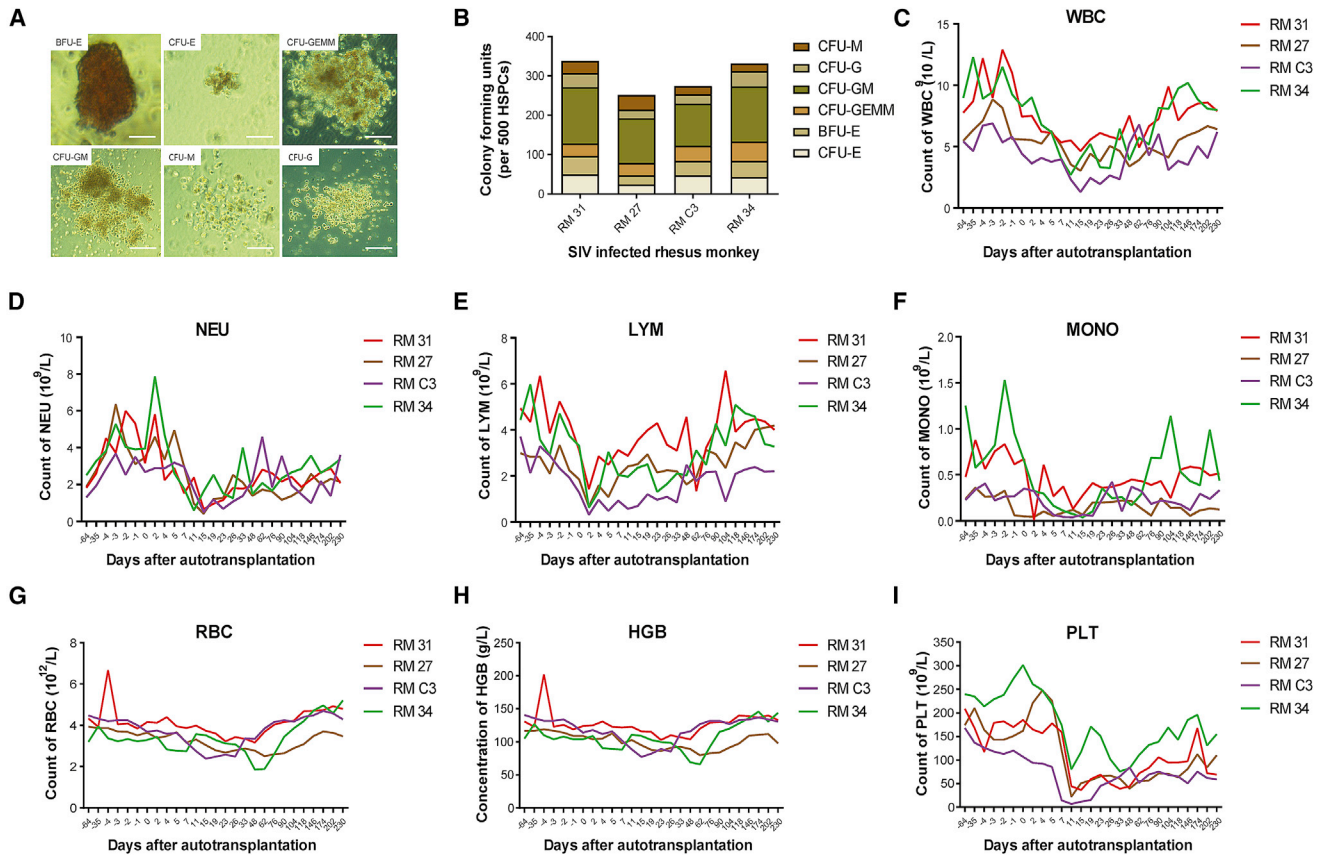


Figure 3. The *In Vitro* Multilineage Potential of *CCR5*-Disrupted HSPCs and the *In Vivo* Dynamics of Different Hematopoietic Cell Subsets
 (A) Representative pictures of six types of colonies formed in methylcellulose: burst-forming unit-erythroid (BFU-E), CFU-erythroid (CFU-E), CFU-granulocyte/macrophage (CFU-GM), CFU-granulocyte (CFU-G), CFU-macrophage (CFU-M), and CFU-granulocyte, erythrocyte, macrophage, megakaryocyte (CFU-GEMM). (B) The quantified data on colony number and types in (A) are presented. Scale bars, 100 μ m. (C–F) The absolute counts of different peripheral karyocytes were recorded before and after transplantation: (C) white blood cell, (D) neutrophil, (E) lymphocyte, and (F) monocyte. (G–I) The erythroid hemocytes and relevant parameters in peripheral blood were tested prior to and after transplantation: (G) red blood cell, (H) hemoglobin, and (I) platelet.

recover rapidly in 3 days. However, 4–5 days posttransplantation, NEU number began to reduce gradually until 2 weeks after engraftment. Then, up to 7 months after transplantation, NEU counts still failed to reach the pretransplantation level, indicating that the number of hematopoietic reconstituted cells was insufficient or some of the engrafted HSPCs were incompetent (Figure 3D). For other types of leukocytes, the number of lymphocytes (LYMs) also declined rapidly after the injection of busulfan, but began to recover and returned to the pretransplant level 2 weeks after transplantation (Figure 3E). The changes in monocytes (MONOs) before and after transplantation were similar to those in LYMs, and the MONO counts of four recipients had recovered to the pretransplant level after 6 months of engraftment (Figure 3F). For the erythroid hematopoietic compartment, the number of red blood cells (RBCs) (Figure 3G), as well as the hemoglobin (HGB) (Figure 3H), of all the monkeys showed a decline after busulfan administration, which lasted for 4–6 weeks after transplantation and then began to recover gradually, especially when monkeys were supportively transfused RBC suspension prepared from healthy monkeys of the same blood type. Notably, the absolute count of platelets (PLTs) decreased sharply

upon busulfan administration and recovered slowly to half of the level before transplantation (Figure 3I). Thus, after autologous HSPC transplantation, SIV-infected monkeys have basically achieved hematopoietic reconstruction, except for the slow recovery of NEUs and PLTs.

The Serum Biochemical Parameters of SIV-Infected Monkeys prior to and after Transplantation of *CCR5*-Modified HSPCs

To assess the physiological status of the monkeys during the transplant and thereafter, we measured the body weight and biochemical indicators. After transplantation, the body weight of monkey RM 31, RM C3, and RM 34 experienced a remarkable reduction and gradually recovered to normal level approximately 1 month later. For animal RM 27, weight loss lasted during ART treatment and was not improved to the last observation (Figure 4A). Overall, the loss of body weight was combined with the presence of symptoms such as diarrhea and cough (data not shown).

The biochemical parameters tested in the blood include: alanine aminotransferase (ALT) (Figure 4B), aspartate aminotransferase

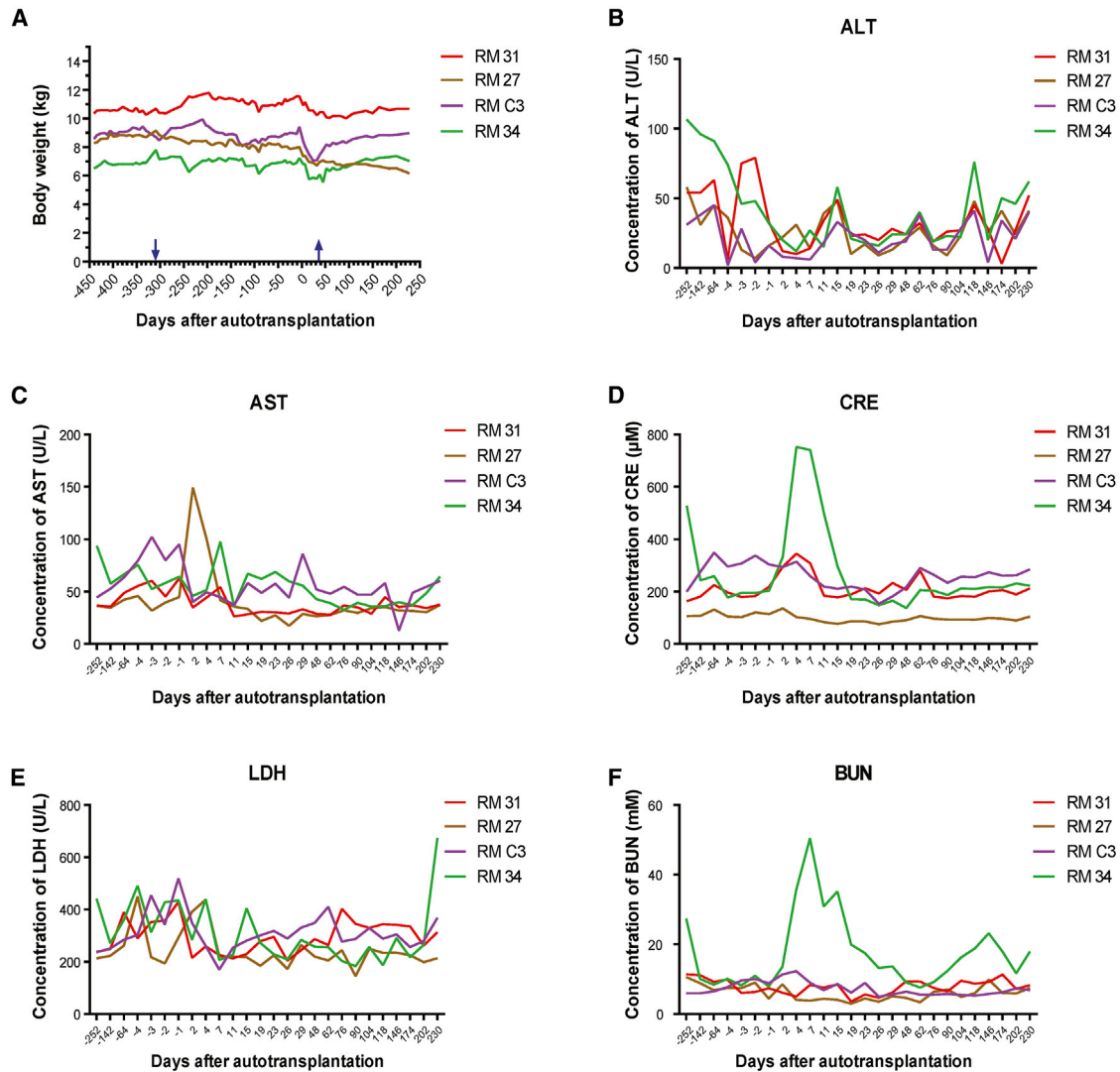


Figure 4. The Body Weight and Serum Biochemical Results of SIV-Infected Monkeys prior to and after Transplantation of Autologous *CCR5*-Modified HSPCs

(A) The changes in the body weight of experimental monkeys before and after transplantation. The blue arrows indicate the start (arrow up) and stop (arrow down) of ART treatment. (B–F) The changes in the serum biochemical parameters of SIV-infected monkeys before and after engraftment: (B) alanine aminotransferase, (C) aspartate aminotransferase, (D) creatinine, (E) lactate dehydrogenase, and (F) urea nitrogen.

(AST) (Figure 4C), creatinine (CRE) (Figure 4D), lactate dehydrogenase (LDH) (Figure 4E), and urea nitrogen (BUN) (Figure 4F); each detection index has its physiological significance. ALT and AST mainly indicate whether liver function is abnormal, CRE and BUN mainly indicate whether kidney function is abnormal, and LDH is related to the function of the heart. For RM 34 monkey, BUN and CRE values peaked about 2 weeks after transplantation and then gradually decreased, but then increased again, suggesting that this monkey may have glomerular filtration dysfunction (Figures 4D and 4F). Other monkeys did not show obvious abnormalities in their overall physiology, despite fluctuations in certain parameters.

The Level of *CCR5* Gene Editing *In Vivo* after Transplantation

Lymphoid tissues, especially gut-associated lymphoid tissues, are major HIV-1 replication sites. To characterize the trafficking and behavior of *CCR5*-disrupted cells at tissue level, we collected the peripheral lymphoid tissues (inguinal lymph node) at different time points before and after transplantation, and the gastrointestinal (GI) biopsies from upper GI (duodenum) and lower GI (colon) were collected as previously described.²⁹ The above samples were subjected to the assessment of *CCR5* knockout efficiency as described previously.²⁵ There was a weak enrichment of *CCR5*-deficient cells in inguinal lymph nodes (ranging from 1% to 1.5%) after transplant (Figure 5A). For upper GI tissues, the percentage of *CCR5*-disrupted

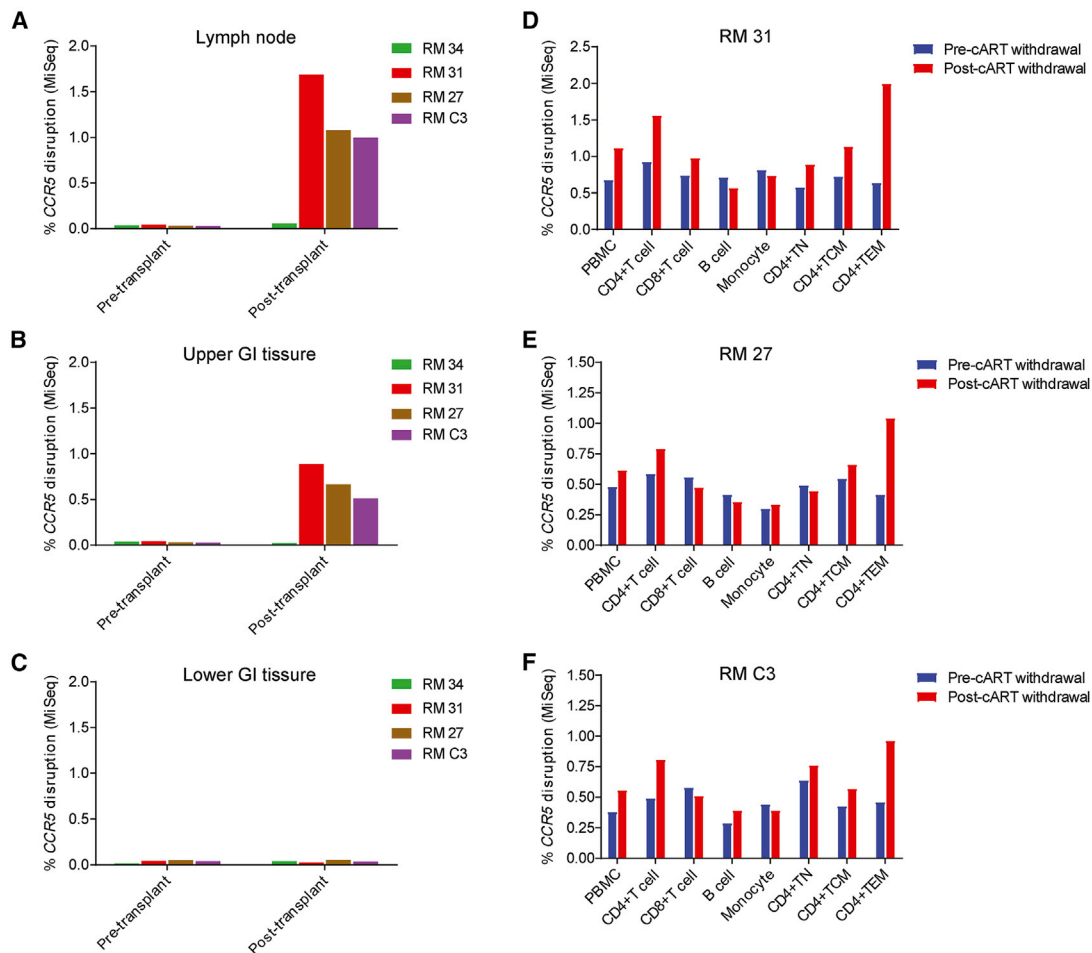


Figure 5. The Level of *CCR5* Gene Editing *In Vivo* after Transplantation of Autologous *CCR5*-Modified HSPCs

(A–C) The efficiency of *CCR5* disruption in peripheral lymph node (A), upper GI tissue (duodenum) (B), and lower GI tissue (colon) (C) at different time points. The pre-transplant and post-transplant dates are 64 days before transplant and 174 days after transplant, respectively. (D–F) The rates of *CCR5* gene disruption in different hematopoietic cell types (PBMC, CD4⁺ T cell, CD8⁺ T cell, B cell and monocyte, CD4⁺ TN, CD4⁺ TCM, and CD4⁺ TEM) in three monkeys who received transplantation of autologous *CCR5*-disrupted HSPCs: RM31 (D), RM27 (E), and RM C3 (F) at indicated dates. The pre- and post-combination ART (cART) withdrawal dates are 33 and 202 days after transplant, respectively.

cells was around 0.6%–1% (Figure 5B). By contrast, the disruption of *CCR5* gene in lower GI samples was hardly detected after transplant (Figure 5C). Then we stepped forward to assay the rates of *CCR5* gene disruption in different hematopoietic cell types in peripheral blood. The frequencies of *CCR5* gene disruption in different hematopoietic cell subsets (peripheral blood mononuclear cell [PBMC], CD4⁺ T cell, CD8⁺ T cell, B cell, and MONO) range from 0.3% to 1.1% before the cessation of ART (Figures 5D–5F). However, the ratios of *CCR5*-edited cells in CD4⁺ T cells were uniformly increased ~120 days post-ART withdrawal. Especially in the CD4⁺ TEM subgroup, the *CCR5*-disrupted cells were dramatically enriched (3.1-fold for RM 31, 2.5-fold for RM 27, and 2.1-fold for RM C3) 8 months after ART withdrawal (Figures 5D–5F). By contrast, the percentages of *CCR5*-disrupted cells in CD4⁺ Central Memory T cell (TCM) and CD4⁺ Naïve T cell (TN) subsets were not significantly increased after viral rebound (Figures 5D–5F). These results

together with earlier research indicated that part of CD4⁺ T cells that derived from *CCR5*-disrupted HSPCs could persist *in vivo* and undergo the virus-dependent positive selection.²⁶

Because the lentivirus system was used to deliver the CRISPR/Cas9 system in this study, we evaluated the expression of Cas9 and guide RNAs at different time points after transplant. For all the CRISPR/Cas9-treated animals, the expression level of Cas9 protein declined remarkably with time (Figure S2A). Similarly, the relative expression of guide RNAs in three *CCR5*-modified monkeys was uniformly reduced over time (Figure S2B). Nevertheless, the residual Cas9 protein and guide RNAs remained detectable up to 8 months after transplantation.³⁰ The off-target effects of CRISPR were measured based on the deep-sequencing platform, and no obvious off-target events were detected (Figures S2C and S2D).²⁵

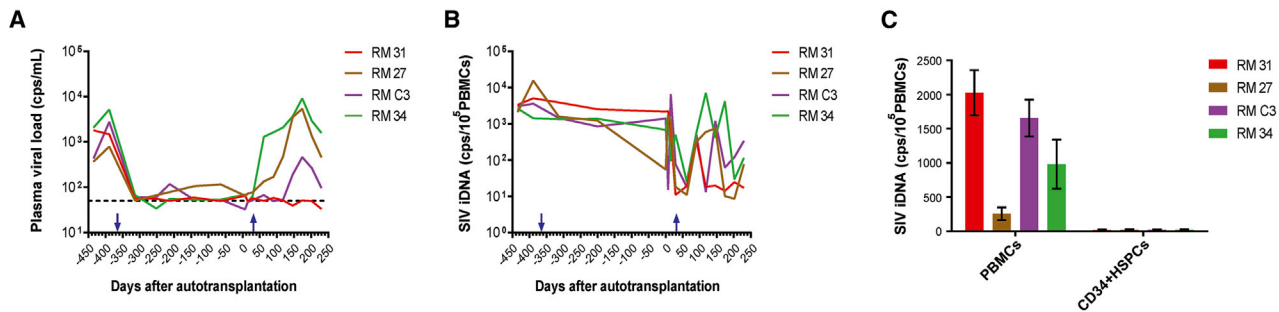


Figure 6. The SIV Viral Load before and after Transplantation of Autologous CCR5-Modified HSPCs

(A) The changes of SIV RNA in plasma before and after transplantation. (B) The changes of SIV iDNA in PBMCs pre- and post-engraftment. The up arrow and down arrow indicate the start and stop of ART treatment, respectively. (C) The quantification of SIV iDNA in PBMCs and purified CD34⁺ HSPCs collected from SIV-infected monkeys ~127 days before transplant. Data are expressed as mean \pm SD.

The Impact of Autograft of CCR5-Disrupted HSPCs on Peripheral SIV Viral Load

As shown in Figure 1, after monkeys had entered the plateau stage of SIV infection, ART was launched and strongly reduced the plasma viral load of all the animals (Figure 6A). The extent of hematopoietic reconstruction in this study was assessed by the percentage of reticulocytes in peripheral blood (data not shown).³¹ When engraftment was successful, the ART drugs were withdrawn. Monkeys RM 27 and RM 34 showed a rapid and complete rebound of plasma SIV 1 week after ART cessation (Figure 6A). However, monkey RM C3 showed a slow and moderate rebound of plasma SIV 3 months after withdrawal of ART (Figure 6A). In particular, for monkey RM 31, the plasma viral load dropped drastically since the start of ART (from the peak value of 1,500 copies [cps]/mL to ~50 cps/mL) and remained undetectable for over 7 months after cessation of ART (Figure 6A).^{32,33}

We also analyzed the integrated SIV virus (SIV iDNA) in PBMCs of experimental monkeys before and after transplantation. The copy number of SIV iDNA decreased slowly during the whole process of ART (Figure 6B). SIV iDNA was reduced significantly because of busulfan's effect in scavenging bone marrow cells and some peripheral LYMs. After cessation of ART, the SIV iDNA rapidly recovered probably because of the non-myeloablative dosage of busulfan and rebound of plasma virus. Subsequently, the SIV iDNA copy number of the four monkeys showed different changes. The SIV iDNA copy number for RM 31 was kept at a low level corresponding to its enrichment of CCR5-disrupted cells in peripheral CD4⁺ T cells (Figure 5D). The other two monkeys with CCR5 modification (RM 27 and RM C3) together with RM 34, which did not experience the CRISPR/Cas9 modification, maintained a high number of SIV iDNA copies with some fluctuation (Figure 6B).

An important concern is whether HIV-1/SIV could infect HSPCs and establish latent cellular reservoirs,^{34–36} so we detected the SIV iDNA in PBMCs and HSPCs collected from SIV-infected monkeys on ART before transplant. For HSPCs, the number of SIV iDNA copies was

lower than the limit of detection, whereas the PBMCs collected at the same time contained multiple copies of SIV iDNA (Figure 6C). These results suggested that long-term ART regimen could control viral load and inhibit the SIV infection of CD34⁺ HSPCs in bone marrow.

The Effect of Transplant of Autologous CCR5-Disrupted HSPCs on CD4⁺ T Cell Count and the Expression of CCR5

Before ART treatment, SIV monkeys were in the period of chronic infection with the absolute count of CD4⁺ T cells above 500 cells/ μ L. All of the animals showed increased and relatively stable counts of CD4⁺ T cells during ART treatment. For monkey RM 31, CD4⁺ T cell count reached 1,200 cells/ μ L before ART (Figure 7A) and remained high until conditioning and transplantation. When hematopoietic mobilization was performed and PBMCs were collected by apheresis, the absolute counts of CD4⁺ T cells showed a decreasing trend from the second collection of HSPCs 4 months before the operation and declined to the nadir after the injection of busulfan (Figure 7A). The number of CD4⁺ T cells began to recover after the hematopoiesis was basically restored. After termination of ART, the CD4⁺ T cell counts of four SIV monkeys declined transiently before returning to the level during ART treatment, and the CD4 absolute count of RM 31 was superior to other monkeys (Figure 7A). The changes of CD4/CD8 ratio also reflected the level of immune balance in the monkeys. Following a sharp decline shortly after cessation of ART, the CD4/CD8 ratio in monkey RM 31 gradually recovered to the level during ART treatment (Figure 7B).

Because SIVmac251 uses CCR5 as the major co-receptor for entry into monkey CD4⁺ T cells,³⁷ we examined the expression of CCR5 in CD4⁺ T cells. During ART treatment, the expression level of CCR5 in CD4⁺ T cells was significantly increased for all of the SIV-infected monkeys. However, the proportion of CCR5⁺CD4⁺ T cells decreased after termination of ART 1 month after transplantation (Figure 7C). A possible explanation is that, in the absence of antiviral drugs, a large number of free SIVs in peripheral blood could infect and lead to the death of CCR5⁺CD4⁺

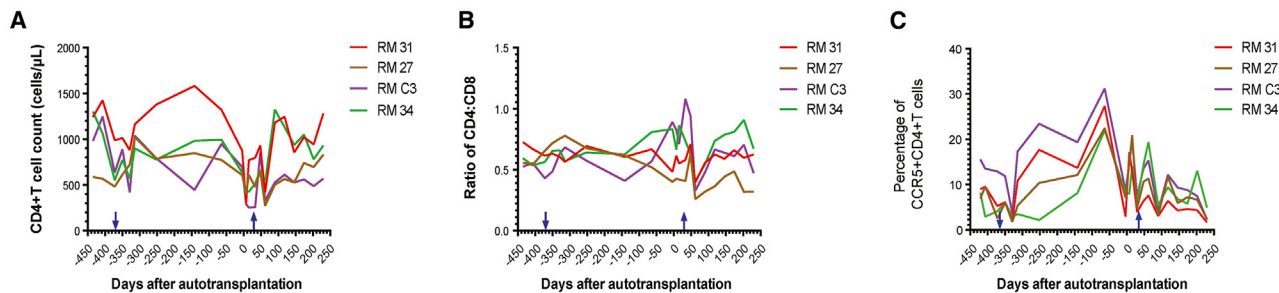


Figure 7. The Absolute Count of Peripheral CD4⁺ T Cells, and the Expression of CCR5 before and after Autotransplantation of CCR5-Modified HSPCs
 (A) The changes of circulating CD4⁺ T cell count pre- and post-transplantation. (B) The changes in peripheral CD4/CD8 ratio before and after engraftment. (C) The proportion of CCR5⁺CD4⁺ T cells in whole circulating CD4⁺ T cells prior to and after transplantation. The blue arrows in (A)–(C) indicate the start (arrow up) and stop (arrow down) of ART treatment.

T cells. Monkey RM 31 showed the lowest level of CCR5 expression in CD4⁺ T cells (Figure 7C). Nevertheless, the proportion of CCR5⁺CD4⁺ T cells remained low in both the CCR5-modified and control animals, which suggested that modifying CCR5 gene may play only a partial role in CCR5 expression on CD4⁺ T cells.

DISCUSSION

HIV-1 gene therapy has been explored for decades, and there are many new drugs targeting the viral or host genes.^{38,39} In this study, we disrupted the CCR5 gene in HSPCs of SIV-infected rhesus macaques on ART, engrafted the modified autologous HSPCs to the infected monkeys, and assessed the frequency of CCR5 gene editing *in vivo*, SIV viral load, immune function, and sets of physiological parameters.

The adverse effects of this approach observed in this pilot trial include weight loss, diarrhea, emesis, and hair loss, which were mainly caused by the immunosuppressive effect of busulfan.⁴⁰ However, these adverse effects gradually disappeared with the success of engraftment in most animals. In terms of safety, the four subjects all survived the operation of apheresis, autologous transplantation, and ART withdrawal during the observation period. Moreover, long-term follow-up of blood routine and biochemical indicators showed that these monkeys were able to maintain physiological homeostasis after transplantation of HSPCs defective for CCR5.

In the preliminary observation of validity, two (RM 31 and RM C3) of the three treated recipients (2/3) showed delayed SIV rebound, and only one (RM 31; Figure 6A) of them showed undetectable viral rebound until now accompanied by the relatively reduced level of SIV iDNA (Figure 6B). Correspondingly, the immunological markers of monkey RM 31 (absolute count of CD4⁺ T cells, ratio of CD4/CD8 cells, proportion of different types of immune cells) also indicated its immune function was maintained at a relatively high level. Given that some MHC haplotypes in nonhuman primates are able to naturally control infection of SIV, which could, for example, explain the data in RM 31, the experimental monkeys were subjected to the analysis of Mamu haplotypes.⁴¹ It was found that all the animals enrolled

in the current study were negative for Mamu-A*01, Mamu-A*11, Mamu-B*08, and Mamu-B*17, the well-known haplotypes that could play a protective role in SIV-infected monkeys (data not shown).^{41–44} Nevertheless, we acknowledged that it remains difficult to interpret the viral correlates related to the transplantation intervention in RM 31 and RM C3. In spite of some limitations, including low level of gene modification and small sample size, this study together with previous reports confirmed that even at low levels,²⁶ the engraftment of CCR5-disrupted HSPCs may give rise to SIV-resistant CCR5-negative CD4⁺ T cells that have the potential to refill the virus-depleted CD4⁺ T cell niche. Based on the current data, it is hypothesized that a higher efficiency of gene knockout could significantly reduce the proportion of CD4⁺ T cells infected by CCR5-tropic SIV, thereby reducing the viral reservoir in peripheral blood. It will take a longer time for CCR5-ablated HSPCs to yield more SIV-resistant CD4⁺ T cells to realize the state of functional cure. Hence prolonged observation will probably help to further clarify the immune protection against SIV in infected monkeys so as to comprehensively evaluate the role of CCR5 modification in controlling viral infection and maintaining immune balance.

The limitation of this research is that it is only a preliminary study with too few animals and no better control groups (transplantation of HSPCs in healthy monkeys and transplantation of unmodified HSPCs in SIV-infected monkeys) were included, so it is impossible to draw conclusions from the current results. Meanwhile, the knockout efficiency of CCR5 gene needs to be further improved, and the experimental design needs to be further optimized. Therefore, emphasis should be placed on the need for a well-designed *in vivo* study of rhesus monkeys with the necessary control groups before conducting clinical trials.

Individuals infected with HIV-1 frequently show cytopenia and suppressed hematopoiesis; however, the role of direct HIV-1 infection of HSPCs in this process remains controversial.^{34,35,45} It has been documented that HIV-1 can infect hematopoietic progenitor cells (HPCs) using CXCR4 receptors.³⁵ However, the CD34⁺ cells obtained by leukapheresis and purification are a mixture of HSCs and HPCs. To our surprise, the current data showed that the copy

number of SIV iDNA in these mixed hematopoietic cells was lower than the detection threshold of the Alu-PCR, suggesting that there were few latent proviruses in HSPCs here. This may be because long-term ART drugs inhibited the replication of SIV in peripheral blood, thus protecting HSPCs in bone marrow from infection of SIV,³⁶ which is crucial for rebuilding a fully protective immune system after reconstruction.

Given the late time to initiate ART, some animals already displayed multiple organ infections (data not shown), so the therapeutic effect of ART is not optimal. Although the absolute count of CD4⁺ T cells did not fall to the reference level of AIDS (below 200/μL),⁴⁶ the monkeys showed increasing collapse of protective immunity, which adversely affected the mobilization of HSPCs and the reconstitution of immune function. Therefore, repeated trials that extensively evaluate the levels of viral infection and immune function of monkeys should be conducted before carrying out HSPC-based gene therapy in the future.

MATERIALS AND METHODS

Animals and the Experimental Design

The Chinese rhesus macaques (*Macaca mulatta*) were housed and fed according to guidelines established by the *Guide for the Care and Use of Laboratory Animals* and the Animal Welfare Act at the Non-human Primate Animal Center of the Guangzhou Institutes of Biomedicine and Health (GIBH). The animal experiments performed in this study were approved by the GIBH Institutional Animal Care and Use Committee. **Figure 1** shows the study design, and **Table S1** shows the information and treatments of animals. All monkeys were inoculated with SIVmac251 (10⁴ median tissue culture infective dose [TCID₅₀]) and treated with ART for over 1 year. The ART regimen included 9-R-(2-phosphonomethoxypropyl) adenine (PMPA) (30 mg/kg; Desano Pharmaceuticals, Shanghai, China) and emtricitabine (FTC) (20 mg/kg; Desano Pharmaceuticals, Shanghai, China), administered once daily intramuscularly (i.m.). During the ART treatment, the recombinant human SCF (100 μg/kg/day; PeproTech, Rocky Hill, NJ, USA) and G-CSF (25 μg/kg/day; PeproTech, Rocky Hill, NJ, USA) were injected subcutaneously to the SIV-infected monkeys for 3–5 consecutive days followed by apheresis operation. Two collections of CD34⁺ HSPCs were pooled together and infected with CCR5-specific CRISPR/Cas9 lentiviruses. Prior to engraftment of autologous CD34⁺ HSPCs (day 0), each monkey was intravenously infused with busulfan (80 mg/cm² surface area) (Busulfex; Kyowa Hakko Kirin Pharmaceutical, Shanghai, China) at the speed of 0.1 mL/min on days –4 and –2 according to previous research.⁴⁷ RBCs with the same blood type (group B and AB) were infused to recipients to prevent anemia. The extent of hematopoietic reconstitution was assessed by the percentage of reticulocytes in peripheral blood.³¹ About 1 month later, the engraftment was successful and ART treatment was terminated. The body weight, blood routine, blood biochemistry, and virological and immunological indexes of experimental monkeys at different time points were measured to evaluate the safety and efficacy of this animal model.

Quantification of SIV RNA in Plasma and Integrated SIV DNA in PBMCs

The levels of plasma SIV RNA were measured by quantitative reverse-transcriptase PCR (qRT-PCR), as previously described.²² The amount of SIV iDNA integrated in PBMCs was quantified using modified Alu-PCR according to the previous method.^{22,48} All of the primers and probes for the above qRT-PCR and Alu-PCR were listed in **Figure S1**.

HSPCs Culture and Transfection with SIV-R5-H or SIV-R5-HI

The SIV-infected macaques received SCF (100 μg/kg/day; Amgen, Thousand Oaks, CA, USA) and G-CSF (25 μg/kg/day; Amgen, Thousand Oaks, CA, USA) as subcutaneous injections for 3 days. Mobilized peripheral blood cells were collected by apheresis on day 3 as described previously.⁴⁹ Mononuclear cells were isolated using density gradient centrifugation over LYM separation medium (Organon Teknika, Durham, NC, USA), and enrichment of CD34⁺ cells was performed using a Dynabeads CD34⁺ isolation kit (Invitrogen, Carlsbad, CA, USA) per the manufacturer's instruction. The purity of CD34⁺ cell sorting was around 75%. For each animal, the apheresis was conducted twice at different time points to harvest more HSPCs for transplantation. The CD34⁺ cells collected from two batches were pooled together and pre-stimulated for 24 h with SCF, Flt3-L, and thrombopoietin [TPO] (100 ng/mL for each; PeproTech, Rocky Hill, NJ, USA) on RetroNectin (Takara, Shiga, Japan)-coated plates. Then the cells were exposed to SIV-GFP, SIV-R5-H, or SIV-R5-HI infection (MOI = 100) supplemented with 8 μg/mL Polybrene (Sigma-Aldrich, St. Louis, MO, USA) for 8 h and then transferred into fresh medium containing cytokines and vector particles, and incubation was continued for another 12 h. A fraction of infected HSPCs was retained to analyze the efficiency of CCR5 gene modification and assess the potential of hematopoietic differentiation.

Colony-Forming Cell Assay

One thousand sorted CD34⁺ HSPCs were plated in 3 mL methylcellulose (MethoCult H4435 Enriched; STEMCELL Technologies) on a 35-mm cell culture dish and cultured for 2 weeks at 37°C in a 5% CO₂ incubator. Different categories of colonies were then counted and scored.

Construction of SIV Lentiviral Vectors: pCL-CAS-sgR5-H and pCL-CAS-sgR5-HI

The SIV-based lentiviral vector (pCL20c-SLFR-MSCV-GFP) and the packaging system (pCAG-SIVgprre, pCAG4-RTR-SIV, and pCAG-VSV-G) were generous gifts from Dr. Nienhuis. The optimal sgRNAs targeting monkey CCR5 gene (GenBank: NM_001042773.3) locus (sgR5-H and sgR5-I) have been reported in our previous research.¹⁹ For the single-guide RNA expression vector, the hU6-sgR5-H-EFS-spCas9-puro cassette was PCR amplified from pLenti-CAS-sgR5-H and then inserted into the HpaI/ClaI (NEB, Ipswich, MA, USA)-digested lentiviral vector pCL20c-SLFR-MSCV-GFP to yield a new plasmid: pCL-CAS-sgR5-H. For the dual-guide RNA expression vector, the hU6-sgR5-I cassette was PCR amplified from pLenti-CAS-

sgR5-I and then tandemly linked with the 3' end of the sgR5-H sequence of EcoRI (NEB)-digested pCL-CAS-sgR5-H. This new plasmid was named pCL-CAS-sgR5-HI. All of the sgRNA target sites and primer sequences are shown in [Figure S1](#).

Packaging and Purification of CRISPR/Cas9 Lentiviruses: SIV-R5-H and SIV-R5-HI

The production of SIV-based lentiviruses was performed as previously described.²⁸ In brief, 1×10^7 HEK293T cells (ATCC, Gaithersburg, MD, USA) were seeded onto 145-mm Petri dishes in Dulbecco's modified Eagle's medium (DMEM; GIBCO, Carlsbad, CA, USA) containing 10% fetal bovine serum (FBS; DF-10; GIBCO) and containing 100 U/mL penicillin G (Sigma-Aldrich) and 100 µg/mL streptomycin (Sigma-Aldrich). Twenty-four hours later, cells were transfected with a total of 42 µg DNA composed as follows: 9 µg pCAG-SIVgprre, 9 µg pCAG4-RTR-SIV, 9 µg pCAG-VSV-G, and 15 µg pCL-CAS-sgR5-H or pCL-CAS-sgR5-HI. Transfection was performed using linear PEI_{max} (Polysciences, Warrington, PA, USA) according to our previous study.¹⁹ After 8 h, the media were replaced with 20 mL of serum-free UltraCULTURE (Lonza, Basel, Switzerland) medium supplemented with 0.6 mg/mL glucose (Sigma-Aldrich) and 1% GlutaMAX (GIBCO). After another 60 h, all of the cell supernatant was collected and centrifuged at $500 \times g$ at 25°C for 10 min to pellet the cell debris, and the supernatant was filtered through a 0.45-µm low protein binding membrane (Merck Millipore, Darmstadt, Germany). To achieve a 300× concentration of the CRISPR/Cas9 lentiviruses, the filtered medium containing virions was ultracentrifuged at 20,000 rpm for 2 h at 4°C, resuspended in PBS without Ca²⁺ and Mg²⁺ overnight at 4°C, snap frozen in aliquots, and stored at -80°C.

Titration of SIV-R5-H and SIV-R5-HI Based on the Number of Vector Copies Integrated into Cellular Genome

To determine the titer of concentrated lentiviruses, we used a previously reported quantitative PCR method with some modifications in primers and probe.¹⁹ The SIV lentiviral shuttle vector originated from the SIVmac1A11 strain. For the SIV Gag detection, the primer pair and the probe were listed in [Figure S1](#).

NHEJ Assay and Deep Sequencing for Genome Mutagenesis

The genomic DNA was extracted from modified and control cells using a DNeasy Blood & Tissue Kit (QIAGEN, Dusseldorf, Germany). After PCR amplification of the CCR5 sgRNA binding sites by Phanta Max Super-Fidelity DNA Polymerase (Vazyme, Nanjing, China) with the gene-specific primers listed in [Figure S1](#), the Cruiser Gene Knockout Detection Kit (Genloci Biotechnologies, Nanjing, China) was used according to the manufacturer's instructions. The digested DNA was resolved by 12% PAGE on the Gel Imaging System. The ratio of cleaved to un-cleaved products was calculated as a measure of frequency of gene modification using ImageJ software (NIH Image-BioLab).⁵⁰ To detect the efficacy of gene editing *in vivo*, we quantified the percentage of CCR5-edited alleles in each sample using the Illumina MiSeq platform according to previous research.²⁵

Lymph Node Collections, Gut Biopsies, Blood Cell Sorting, and Flow Cytometry

At the indicated time points, inguinal lymph nodes were collected and flash frozen. GI biopsies from upper GI (duodenum) and lower GI (colon) were collected as described previously.²⁹ Single-cell suspensions were prepared from cell culture or peripheral tissues. Peripheral blood cell subsets were sorted using magnetic bead kits from Miltenyi Biotec (Bergisch Gladbach, Germany) or through antibody labeling and a FACSAria II machine (BD Biosciences, Franklin Lakes, NJ, USA). The following antibodies (clones) were purchased from BD Biosciences: CD3 (SP34-2), CD4 (L200), CD45 (D058-1283), CCR5 (3A9), CD11b (ICRF44), CD14 (M5E2), CD16 (3G8), CD34 (563), CD28 (CD28.2), and CD95 (DX2). Anti-CD8 (B9.11) and anti-CD19 (J3-119) were purchased from Beckman Coulter (Brea, CA, USA). Anti-CD38 (AT-1) was purchased from STEMCELL Technologies (Vancouver, BC, Canada). For surface marker measurement, individual antibodies were added to the cell suspension alone or together. Isotype control antibodies were used for gating the positive group of target cells. Cells were stained with antibodies for 20 min at room temperature followed by washing twice with PBS plus 2% FBS. After resuspension, cells were subjected to FACS analysis in less than 8 h.

Routine and Biochemical Blood Tests of Rhesus Macaque

The peripheral blood added with or without anticoagulant was transported at room temperature. The whole blood with anticoagulant was used for blood routine assay of WBC, NEU, LYM, MONO, RBC, PLT, HGB, and hematocrit value (HCT) within 4 h. The whole blood without anticoagulant was first centrifuged, and the upper serum was isolated and frozen at -20°C. The serum biochemical indicators, including ALT, AST, CRE, BUN, and LDH, were tested within 1 month.

Statistical Analysis

All statistical analyses were performed with GraphPad Prism software. Statistical significance was determined with the Mann-Whitney *U* test, with $p < 0.05$ considered statistically significant. Data are presented as mean \pm SD.

SUPPLEMENTAL INFORMATION

Supplemental Information can be found online at <https://doi.org/10.1016/j.omtm.2020.03.004>.

AUTHOR CONTRIBUTIONS

S.Y., Y.Y., and X.C. conceived and designed the project. S.Y., Y.O., H.X., J.L., and Y.Y. performed the experiments and analyzed the data. S.L., S.Z., and L.Q. provided technical assistance. S.Y., Y.O., and Y.Y. contributed to manuscript preparation. D.A. helped to revise the manuscript. X.C. wrote the manuscript and supervised the whole project.

CONFLICTS OF INTEREST

The authors declare no competing interests.

ACKNOWLEDGMENTS

We thank Prof. Arthur W. Nienhuis (St. Jude Children's Research Hospital) for kindly providing pCL20c-SLFR-MSCV-GFP, pCAG-SIVgprre, pCAG4-RTR-SIV, and pCAG-VSV-G plasmids. We sincerely thank Weimin Zhang, Jianfu Tao, and Xiangjie Feng for the help of handling the experiments on rhesus macaques. We also thank Zhoufang Li and Quan Liu for their support in deep sequencing technology and data processing. This work was supported by the National Key R&D Program of China (grant 2016YFE0107300); the National Natural Science Foundation of China (grants 81673003 and 31570925); the Science and Technology Service Network Project of Chinese Academy of Sciences (grant KFJ-ST-S-QYZX-042); the Hunan Provincial Key Laboratory of Dark Tea and Jin-hua (grant 2016TP1022); and the Science and Technology Program of Guangzhou, China (grant 201707010447).

REFERENCES

- Hütter, G., Nowak, D., Mossner, M., Ganepola, S., Müssig, A., Allers, K., Schneider, T., Hofmann, J., Kücherer, C., Blau, O., et al. (2009). Long-term control of HIV by CCR5 Delta32/Delta32 stem-cell transplantation. *N. Engl. J. Med.* *360*, 692–698.
- Allers, K., Hütter, G., Hofmann, J., Lodenkemper, C., Rieger, K., Thiel, E., and Schneider, T. (2011). Evidence for the cure of HIV infection by CCR5Δ32/Δ32 stem cell transplantation. *Blood* *117*, 2791–2799.
- Gupta, R.K., Abdul-Jawad, S., McCoy, L.E., Mok, H.P., Peppas, D., Salgado, M., Martinez-Picado, J., Nijhuis, M., Wensing, A.M.J., Lee, H., et al. (2019). HIV-1 remission following CCR5Δ32/Δ32 haematopoietic stem-cell transplantation. *Nature* *568*, 244–248.
- Huang, Y., Paxton, W.A., Wolinsky, S.M., Neumann, A.U., Zhang, L., He, T., Kang, S., Ceradini, D., Jin, Z., Yazdanbakhsh, K., et al. (1996). The role of a mutant CCR5 allele in HIV-1 transmission and disease progression. *Nat. Med.* *2*, 1240–1243.
- Deng, H., Liu, R., Ellmeier, W., Choe, S., Unutmaz, D., Burkhart, M., Di Marzio, P., Marmor, S., Sutton, R.E., Hill, C.M., et al. (1996). Identification of a major co-receptor for primary isolates of HIV-1. *Nature* *381*, 661–666.
- Allers, K., and Schneider, T. (2015). CCR5Δ32 mutation and HIV infection: basis for curative HIV therapy. *Curr. Opin. Virol.* *14*, 24–29.
- Martinson, J.J., Chapman, N.H., Rees, D.C., Liu, Y.T., and Clegg, J.B. (1997). Global distribution of the CCR5 gene 32-basepair deletion. *Nat. Genet.* *16*, 100–103.
- Pernet, O., Yadav, S.S., and An, D.S. (2016). Stem cell-based therapies for HIV/AIDS. *Adv. Drug Deliv. Rev.* *103*, 187–201.
- Xu, L., Yang, H., Gao, Y., Chen, Z., Xie, L., Liu, Y., Liu, Y., Wang, X., Li, H., Lai, W., et al. (2017). CRISPR/Cas9-Mediated CCR5 Ablation in Human Hematopoietic Stem/Progenitor Cells Confers HIV-1 Resistance In Vivo. *Mol. Ther.* *25*, 1782–1789.
- Wang, G., Zhao, N., Berkhout, B., and Das, A.T. (2018). CRISPR-Cas based antiviral strategies against HIV-1. *Virus Res.* *244*, 321–332.
- Pickar-Oliver, A., and Gersbach, C.A. (2019). The next generation of CRISPR-Cas technologies and applications. *Nat. Rev. Mol. Cell Biol.* *20*, 490–507.
- Mandal, P.K., Ferreira, L.M.R., Collins, R., Meissner, T.B., Boutwell, C.L., Friesen, M., Vrbanc, V., Garrison, B.S., Stortchevoi, A., Bryder, D., et al. (2014). Efficient ablation of genes in human hematopoietic stem and effector cells using CRISPR/Cas9. *Cell Stem Cell* *15*, 643–652.
- Xu, L., Wang, J., Liu, Y., Xie, L., Su, B., Mou, D., Wang, L., Liu, T., Wang, X., Zhang, B., et al. (2019). CRISPR-edited stem cells in a patient with HIV and acute lymphocytic leukemia. *N. Engl. J. Med.* *381*, 1240–1247.
- Li, L., He, Z.Y., Wei, X.W., Gao, G.P., and Wei, Y.Q. (2015). Challenges in CRISPR/CAS9 Delivery: Potential Roles of Nonviral Vectors. *Hum. Gene Ther.* *26*, 452–462.
- Aiuti, A., Biasco, L., Scaramuzza, S., Ferrua, F., Cicalese, M.P., Baricordi, C., Dionisio, F., Calabria, A., Giannelli, S., Castiello, M.C., et al. (2013). Lentiviral hematopoietic stem cell gene therapy in patients with Wiskott-Aldrich syndrome. *Science* *341*, 1233151.
- Biffi, A., Montini, E., Lorioli, L., Cesani, M., Fumagalli, F., Plati, T., Baldoli, C., Martino, S., Calabria, A., Canale, S., et al. (2013). Lentiviral hematopoietic stem cell gene therapy benefits metachromatic leukodystrophy. *Science* *341*, 1233158.
- DiGiusto, D.L., Krishnan, A., Li, L., Li, H., Li, S., Rao, A., Mi, S., Yam, P., Stinson, S., Kalos, M., et al. (2010). RNA-based gene therapy for HIV with lentiviral vector-modified CD34(+) cells in patients undergoing transplantation for AIDS-related lymphoma. *Sci. Transl. Med.* *2*, 36ra43.
- Wang, W., Ye, C., Liu, J., Zhang, D., Kimata, J.T., and Zhou, P. (2014). CCR5 gene disruption via lentiviral vectors expressing Cas9 and single guided RNA renders cells resistant to HIV-1 infection. *PLoS ONE* *9*, e115987.
- Yu, S., Yao, Y., Xiao, H., Li, J., Liu, Q., Yang, Y., Adah, D., Lu, J., Zhao, S., Qin, L., and Chen, X. (2018). Simultaneous Knockout of CXCR4 and CCR5 Genes in CD4+ T Cells via CRISPR/Cas9 Confers Resistance to Both X4- and R5-Tropic Human Immunodeficiency Virus Type 1 Infection. *Hum. Gene Ther.* *29*, 51–67.
- Kiem, H.P., Jerome, K.R., Deeks, S.G., and McCune, J.M. (2012). Hematopoietic-stem-cell-based gene therapy for HIV disease. *Cell Stem Cell* *10*, 137–147.
- Evans, D.T., and Silvestri, G. (2013). Nonhuman primate models in AIDS research. *Curr. Opin. HIV AIDS* *8*, 255–261.
- Zhan, X.Y., Wang, N., Liu, G., Qin, L., Xu, W., Zhao, S., Qin, L., and Chen, X. (2014). Plasmodium infection reduces the volume of the viral reservoir in SIV-infected rhesus macaques receiving antiretroviral therapy. *Retrovirology* *11*, 112.
- Nixon, C.C., Mavigner, M., Silvestri, G., and Garcia, J.V. (2017). In Vivo Models of Human Immunodeficiency Virus Persistence and Cure Strategies. *J. Infect. Dis.* *215* (Suppl 3), S142–S151.
- Mavigner, M., Watkins, B., Lawson, B., Lee, S.T., Chahroudi, A., Kean, L., and Silvestri, G. (2014). Persistence of virus reservoirs in ART-treated SHIV-infected rhesus macaques after autologous hematopoietic stem cell transplant. *PLoS Pathog.* *10*, e1004406.
- Peterson, C.W., Wang, J., Norman, K.K., Norgaard, Z.K., Humbert, O., Tse, C.K., Yan, J.J., Trimble, R.G., Shivak, D.A., Rebar, E.J., et al. (2016). Long-term multilineage engraftment of autologous genome-edited hematopoietic stem cells in nonhuman primates. *Blood* *127*, 2416–2426.
- Peterson, C.W., Wang, J., Deleage, C., Reddy, S., Kaur, J., Polacino, P., Reik, A., Huang, M.L., Jerome, K.R., Hu, S.L., et al. (2018). Differential impact of transplantation on peripheral and tissue-associated viral reservoirs: Implications for HIV gene therapy. *PLoS Pathog.* *14*, e1006956.
- Sutherland, D.R., Anderson, L., Keeney, M., Nayar, R., and Chin-Yee, I.; International Society of Hematotherapy and Graft Engineering (1996). The ISHAGE guidelines for CD34+ cell determination by flow cytometry. *J. Hematother.* *5*, 213–226.
- Hanawa, H., Hematti, P., Keyvanfar, K., Metzger, M.E., Krouse, A., Donahue, R.E., Kepes, S., Gray, J., Dunbar, C.E., Persons, D.A., and Nienhuis, A.W. (2004). Efficient gene transfer into rhesus repopulating hematopoietic stem cells using a simian immunodeficiency virus-based lentiviral vector system. *Blood* *103*, 4062–4069.
- Peterson, C.W., Younan, P., Polacino, P.S., Maurice, N.J., Miller, H.W., Prlic, M., Jerome, K.R., Woolfrey, A.E., Hu, S.L., and Kiem, H.P. (2013). Robust suppression of env-SHIV viremia in Macaca nemestrina by 3-drug ART is independent of timing of initiation during chronic infection. *J. Med. Primatol.* *42*, 237–246.
- Hsu, P.D., Scott, D.A., Weinstein, J.A., Ran, F.A., Konermann, S., Agarwala, V., Li, Y., Fine, E.J., Wu, X., Shalem, O., et al. (2013). DNA targeting specificity of RNA-guided Cas9 nucleases. *Nat. Biotechnol.* *31*, 827–832.
- Torres, A., Sánchez, J., Lakomsky, D., Serrano, J., Alvarez, M.A., Martín, C., Valls, C., Nevado, L., Rodríguez, A., Casañó, J., et al. (2001). Assessment of hematologic progenitor engraftment by complete reticulocyte maturation parameters after autologous and allogeneic hematopoietic stem cell transplantation. *Haematologica* *86*, 24–29.
- Suryanarayana, K., Wiltout, T.A., Vasquez, G.M., Hirsch, V.M., and Lifson, J.D. (1998). Plasma SIV RNA viral load determination by real-time quantification of product generation in reverse transcriptase-polymerase chain reaction. *AIDS Res. Hum. Retroviruses* *14*, 183–189.
- Hofmann-Lehmann, R., Swenerton, R.K., Liska, V., Leutenegger, C.M., Lutz, H., McClure, H.M., and Ruprecht, R.M. (2000). Sensitive and robust one-tube real-time reverse transcriptase-polymerase chain reaction to quantify SIV RNA load: comparison of one- versus two-enzyme systems. *AIDS Res. Hum. Retroviruses* *16*, 1247–1257.

34. Carter, C.C., Onafuwa-Nuga, A., McNamara, L.A., Riddell, J., 4th, Bixby, D., Savona, M.R., and Collins, K.L. (2010). HIV-1 infects multipotent progenitor cells causing cell death and establishing latent cellular reservoirs. *Nat. Med.* *16*, 446–451.
35. Carter, C.C., McNamara, L.A., Onafuwa-Nuga, A., Shackleton, M., Riddell, J., 4th, Bixby, D., Savona, M.R., Morrison, S.J., and Collins, K.L. (2011). HIV-1 utilizes the CXCR4 chemokine receptor to infect multipotent hematopoietic stem and progenitor cells. *Cell Host Microbe* *9*, 223–234.
36. Durand, C.M., Ghiaur, G., Siliciano, J.D., Rabi, S.A., Eisele, E.E., Salgado, M., Shan, L., Lai, J.F., Zhang, H., Margolick, J., et al. (2012). HIV-1 DNA is detected in bone marrow populations containing CD4+ T cells but is not found in purified CD34+ hematopoietic progenitor cells in most patients on antiretroviral therapy. *J. Infect. Dis.* *205*, 1014–1018.
37. Wilson, D.P., Mattapallil, J.J., Lay, M.D., Zhang, L., Roederer, M., and Davenport, M.P. (2007). Estimating the infectivity of CCR5-tropic simian immunodeficiency virus SIV(mac251) in the gut. *J. Virol.* *81*, 8025–8029.
38. Spragg, C., De Silva Felixge, H., and Jerome, K.R. (2016). Cell and gene therapy strategies to eradicate HIV reservoirs. *Curr. Opin. HIV AIDS* *11*, 442–449.
39. de Mendoza, C., Barreiro, P., Benitez, L., and Soriano, V. (2015). Gene therapy for HIV infection. *Expert Opin. Biol. Ther.* *15*, 319–327.
40. Kahl, C.A., Tarantal, A.F., Lee, C.I., Jimenez, D.F., Choi, C., Pepper, K., Petersen, D., Fletcher, M.D., Leapley, A.C., Fisher, J., et al. (2006). Effects of busulfan dose escalation on engraftment of infant rhesus monkey hematopoietic stem cells after gene marking by a lentiviral vector. *Exp. Hematol.* *34*, 369–381.
41. Mühl, T., Krawczak, M., Ten Haaf, P., Hunsmann, G., and Saueremann, U. (2002). MHC class I alleles influence set-point viral load and survival time in simian immunodeficiency virus-infected rhesus monkeys. *J. Immunol.* *169*, 3438–3446.
42. Yant, L.J., Friedrich, T.C., Johnson, R.C., May, G.E., Maness, N.J., Enz, A.M., Lifson, J.D., O'Connor, D.H., Carrington, M., and Watkins, D.I. (2006). The high-frequency major histocompatibility complex class I allele Mamu-B*17 is associated with control of simian immunodeficiency virus SIVmac239 replication. *J. Virol.* *80*, 5074–5077.
43. Loffredo, J.T., Maxwell, J., Qi, Y., Glidden, C.E., Borchardt, G.J., Soma, T., Bean, A.T., Beal, D.R., Wilson, N.A., Rehrauer, W.M., et al. (2007). Mamu-B*08-positive macaques control simian immunodeficiency virus replication. *J. Virol.* *81*, 8827–8832.
44. Caskey, J.R., Wiseman, R.W., Karl, J.A., Baker, D.A., Lee, T., Maddox, R.J., Raveendran, M., Harris, R.A., Hu, J., Muzny, D.M., et al. (2019). MHC genotyping from rhesus macaque exome sequences. *Immunogenetics* *71*, 531–544.
45. Stanley, S.K., Kessler, S.W., Justement, J.S., Schnittman, S.M., Greenhouse, J.J., Brown, C.C., Musongela, L., Musey, K., Kapita, B., and Fauci, A.S. (1992). CD34+ bone marrow cells are infected with HIV in a subset of seropositive individuals. *J. Immunol.* *149*, 689–697.
46. Weiss, R.A. (1993). How does HIV cause AIDS? *Science* *260*, 1273–1279.
47. Tarantal, A.F., Giannoni, F., Lee, C.C.I., Wherley, J., Sumiyoshi, T., Martinez, M., Kahl, C.A., Elashoff, D., Louie, S.G., and Kohn, D.B. (2012). Nonmyeloablative conditioning regimen to increase engraftment of gene-modified hematopoietic stem cells in young rhesus monkeys. *Mol. Ther.* *20*, 1033–1045.
48. Yamamoto, N., Tanaka, C., Wu, Y., Chang, M.O., Inagaki, Y., Saito, Y., Naito, T., Ogasawara, H., Sekigawa, I., and Hayashida, Y. (2006). Analysis of human immunodeficiency virus type 1 integration by using a specific, sensitive and quantitative assay based on real-time polymerase chain reaction. *Virus Genes* *32*, 105–113.
49. Donahue, R.E., Kirby, M.R., Metzger, M.E., Agricola, B.A., Sellers, S.E., and Cullis, H.M. (1996). Peripheral blood CD34+ cells differ from bone marrow CD34+ cells in Thy-1 expression and cell cycle status in nonhuman primates mobilized or not mobilized with granulocyte colony-stimulating factor and/or stem cell factor. *Blood* *87*, 1644–1653.
50. Guschin, D.Y., Waite, A.J., Katibah, G.E., Miller, J.C., Holmes, M.C., and Rebar, E.J. (2010). A rapid and general assay for monitoring endogenous gene modification. *Methods Mol. Biol.* *649*, 247–256.